A FEASIBILITY STUDY ON THE CONTROL OF A GENERIC AIR VEHICLE USING CONTROL MOMENT GYROS

Kyong B. Lim* and Daniel D. Moerder†
NASA Langley Research Center
Hampton, Virginia, USA 23681

Abstract

This paper examines feasibility and performance issues in using Control Moment Gyroscopes (CMGs) to control the attitude of a fixed-wing aircraft. The paper describes a control system structure that permits allocating control authority and bandwidth between a CMG system and conventional aerodynamic control surfaces to stabilize a vehicle with neutral aerodynamic stability. A simulation study explores the interplay between aerodynamic and CMG effects, and indicates desirable physical characteristics for a CMG system to be used for aircraft attitude control.

1 Introduction

The use of CMGs to control spacecraft through internal angular momentum exchanges has been established practice for decades. These control effectors operate through internal angular momentum exchanges between the CMGs and the vehicle that contains them. For each torque exerted by the CMG on the spacecraft, an equal and opposite one is exerted on the rotating components of the CMG. As such, CMGs are best suited for providing control when there is no long-term bias in the torque command. When such a bias does exist, angular momentum – opposite to that commanded for the vehicle – builds up in the CMG system, ultimately saturating it as a control effector. This necessitates the occasional application of an external torque to the system to remove the CMGs' built-up angular momentum. In spacecraft, this is often done using reaction jets – a measure that depletes propellant and limits the spacecraft's useful life.

For spacecraft, the motivation for using CMGs has been that they are an efficient means of generating large and precise control torques without using reaction jets (except during desaturation operations). What, other than novelty, motivates applying CMGs to the control of fixed-wing aircraft? The core motivation for using internal momentum transfer devices, such as CMGs, in aircraft is to improve their attitude stability robustness, mitigating uncertainties such

*Senior Research Engineer, Dynamic Systems and Control Branch, kyong.b.lim@nasa.gov
†Senior Research Engineer, Dynamic Systems and Control Branch, d.d.moerder@larc.nasa.gov

as atmospheric disturbances, sudden changes in mass properties, and unsteady aerodynamics that might be induced, under extreme circumstances, by the vehicle's aerodynamic control or propulsion systems. CMGs are conceptually well-suited to providing these benefits:

- CMGs generate their torques independent of ambient flow condition. This is both a blessing and a curse. In the former role, their independence of flow means that CMG torques simply are not subject to corruption by atmospheric uncertainties; further, they are fully available in post-stall flight, and under circumstances when normal aerodynamic control effectors might be shaded from amient flow.

- CMGs can, from the control designer's view, be modelled nearly perfectly – A CMG system is merely a collection of gimballed rotating masses, driven by electric motors. Since there's very little uncertainty in a CMG to which a flight control law would have to be robust, the designer can afford to trade away robustness for performance as the authority of the CMG is increased to dominate or supplant the aerodynamic control effectors – assuming that the CMG is physically capable of generating the required torques.

- Atmospheric flight provides "free" opportunities for CMG desaturation. Aircraft are exposed to a very rich moment disturbance environment arising from nonuniform behavior of the ambient air. These random disturbances can potentially be exploited to bleed off momentum. Alternatively, aerodynamic trimming devices can be used for this purpose.

There is also a conceptual challenge:

- CMGs generate their torques independent of ambient flow condition. The forces and moments operating on an aircraft scale with dynamic pressure, while CMG torques scale with flywheel mass. If a CMG system is to provide a given level of torque authority at a high dynamic pressure, it will have to be substantially more massive than one for which the same torque requirment is imposed only at a lower dynamic pressure. The alternative to increasing flywheel mass in achieving a given CMG angular momentum vector is to increase flywheel speed. Technology development for CMG mass reduction will have to focus both on compact, lightweight, flywheels capable of high speed under maneuvering loads, and on the development of bearings that support these loads without undue friction losses.

If CMGs can effectively augment or supplant traditional aerodynamic control effectors, the performance required of the latter would shrink, helping the CMGs "buy their way" into the aircraft design.

This work complements and continues the efforts documented in [1], [2], and [3]. Reference [2] examines using a body-fixed constant-speed flywheel to generate an angular momentum bias in order to improve attitude stiffness and robustness for atmospheric flight, with particular application to near-hovering operation. In particular, the paper describes a closed-form analytic criterion for sizing the magnitude of the bias momentum necessary to achieve a desired maximum level of response to disturbances, for given airframe dynamics. Reference [3] combines the bias momentum flywheel described in [2] with a CMG array arranged in the pyramidal geometry frequently seen in spacecraft practice [4], [5]. The paper presented a novel nonlinear control law that included a Lyapunov-based guarantee of stability.

Here, we exploit an important qualitative characteristic in the physics of CMGs: For the CMG arrays considered in this study, each CMG consists of a constant-speed flywheel mounted in a gimbal that rotates the flywheel normal to its spin axis. The torque output of the device is the cross product of the flywheel angular momentum vector with the gimbal's rotational velocity vector. A CMG produces nothing unless its gimbal is in motion, and the torque output grows with the magnitude of the gimbal rate. This implies that a given CMG is better able to produce a large, but rapidly varying torque history than a large, slowly varying one.

With this in mind, this paper explores the attractiveness of a flight control system for disturbance rejection and stabilization of steady translational flight of a fixed-wing aircraft, in which aerodynamic and CMG control is partitioned on frequency – with the CMGs realizing the higher-frequency portion of the control commands, and the aero surfaces realizing the low frequency part, along with providing desaturation. It will be seen that such an approach to flight control – at least for this category of flight condition – is feasible using CMGs that do not pose an excessive mass burden on the aircraft, and that when they are used, the demands made on the aerodynamic control surfaces diminish to the point where it is reasonable to assume that they could be significantly reduced in size and actuation power.

The next section of this paper describes the simulation study – vehicle model, CMG physical assumptions, and an overview of the flight control law. Section 3 describes cases considered and results, and provides interpretation. Conclusions are given in Section 4. Details of the flight control law are provided in the appendix.

2 Simulation Study Details

This section presents the numerical experiments performed to assess the conceptual attractiveness of employing CMGs to stabilize a fixed-wing aircraft trimmed for steady, wings-level flight, but subjected to substantial atmospheric disturbances. The "substantial" disturbance employed in this study is Dryden "Severe" turbulence [6] with a mean wind speed of 45 knots at 20 ft altitude. In each simulation, the aircraft flies through this three-axis disturbance for 40 seconds.

The aircraft considered is an F16, modelled using Appendix A of [7]. The vehicle is trimmed, using elevator deflection, at two different subsonic flight conditions that are primarily distinguished by low and high dynamic pressures (or $\bar{q}$) – 50 psf and 378 psf, respectively. The aerodynamic coefficient, $C_{L_\alpha} = .002$ was chosen to reflect an instability in the longitudinal motion. The vehicle model is nonlinear, with six degrees of freedom, and includes all aerodynamic phenomena available in [7], including damping coefficients. Actuator dynamics, aero effector deflection and rate limits were neglected. Table 1 displays the details of the low and high $\bar{q}$ trim conditions

The CMG array assumed for this study was a set of four single-gimballed CMGs, arranged in a square pyramidal configuration, in which the axis of gimbal rotation for each CMG is tilted 144° from the aircraft's z-body axis (positive downward.) This configuration was selected because it provides a nearly spherical momentum envelope [4]. Such configurations are attractive for controlling spacecraft, in which there is usually little difference in magnitude between the several principal moments of inertia. For an aircraft such as this F16, in which $I_{zz}/I_{xx} > 5$, it is probable a geometry giving some more ellipsoidal distribution of momentum would make

Parameter	*Low $\bar{q}$ Case*	*High $\bar{q}$ Case*
Dynamic Pressure (psf)	50	378
Altitude (ft)	200	10,000
True Airspeed (knots)	122	389
AOA (deg)	19.2	3.1
Elevator deflection (deg)	-1.1	-4.3

Table 1: Trim settings used in simulation of steady level flight.

more efficient use of the flywheels – but this type of design optimization will be treated in a future paper.

The individual flywheels in the CMG array are assumed identical and were sized to meet the following criteria:

- Flywheel rotational inertia is 0.1% of $(I_{xx})_{\text{F16}}$, where the aircraft's roll axis was selected because it was the principal axis having the smallest moment of inertia.
- The total mass of the CMG array – assumed to be four flywheels – is 2% of the aircraft mass, $(m)_{\text{F16}}$.

These criteria are, obviously, chosen to assure that the CMG system is not an intrusive element of the vehicle's total static mass budget. Combining these criteria without any consideration of materials physics or mechanical design, we infer from $(I_{xx})_{\text{F16}} = 12846Nm^2$ and $(m)_{\text{F16}} = 10358kg$ that each flywheel is realizable as a ring having $r_{\text{FLYWHEEL}} \approx 0.5m$ and weighing a little less than $52kg$. These parameters have no value at all beyond providing an informal "order-of-magnitude" aid to visualing the impact of packaging such a system in an F16. By baselining these physical flywheel properties, various levels of flywheel angular momentum could be selected for the simulations by specifying a flywheel rotational speed. In reality, the flywheel speed would be chosen "as fast as possible" for the available flywheel technology and the flywheel itself would be shrunken to fit the angular momentum requirement. Before leaving description of the CMGs, it should be noted that dynamical effects such as back-EMF in the electric motors and, particularly, flywheel bearing friction have not been modelled in this study.

The flight control law is designed, using feedback linearization, to track a commanded airframe angular velocity, ω_c, expressed in the vehicle's body frame, such that

$$\dot{\omega} = -G_\omega(\omega - \omega_c) \tag{1}$$

where the gain matrix $-G_\omega$ is chosen to be Hurwitz. The command ω_c is, in turn, chosen to be

$$\omega_c = -g(\epsilon)^{-1} G_\epsilon \epsilon \tag{2}$$

where $\epsilon \in \mathcal{R}^{3\times 1}$ is the vector of Modified Rodriguez Parameters (MRPs) [8] that appear in the direction cosine matrix $C_{bt}(\epsilon)$ that rotates from the "trim" – or "target" – frame to the body

frame. In (2), $g(\epsilon)$ is the RHS of the MRPs' governing differential equations, described in the appendix. The gain matrix $-G_\epsilon$ is, again, chosen Hurwitz. This selection of controller ensures

$$\left.\begin{array}{rcl} \epsilon & \rightarrow & 0 \\ \dot{\epsilon} & \rightarrow & 0 \\ \omega & \rightarrow & \omega_c \\ \omega_c & \rightarrow & 0 \end{array}\right\} \qquad t \rightarrow \infty \tag{3}$$

As mentioned in the introduction, this flight control system deliberately takes advantage of the fact that CMG torque scales directly with gimbal speed. Commanding a CMG gimbal through swing histories with high rates improves the instantaneous mass efficiency of the CMG as a producer of torque, but the corresponding rapid rotation of the output vector implies that such peak efficiency is unavilable for low-frequency torque production. In other words, while a CMG system can produce control torques throughout the nonzero portion of the aircraft's disturbance spectrum, it is most efficient in realizing higher-frequency torque commands. Consistent with this physical observation, the total control torque command u_τ produced by the control law for realizing (1) is partitioned into high and low-frequency bands. The high-frequency band is assigned to the CMGs, while the low-frequency part is assigned to the aero control effectors. Command u_τ is divided by

$$\left.\begin{array}{r} \dot{u}_{\text{AERO}} = G_{\text{AERO}}\left(-u_{\text{AERO}} + u_\tau\right) \\ u_{\text{CMG}} = u_\tau - u_{\text{AERO}} \end{array}\right\} \tag{4}$$

where G_{AERO} is the inverse time constant of the low pass filter. This time constant can be used as a design parameter for a given application. For example, a larger participation of CMGs (when working with aero control surface effectors) during disturbance rejection can be specified by using a larger time constant. In the simulation results described in the next section, a time constant of approximately 3 seconds is used to define the case where both CMGs and aero control surfaces are used.

3 Simulation Cases and Results

This section details the simulation cases that were run, and discusses the results. For each of the two flight conditions considered, three control configurations were run: CMGs only, aero control surfaces only, and a combination of CMGs and aero control, using the frequency partitioning filter in (4). These are named in Table 2.

Note that the final column of Table 2 lists flywheel speed for each of these runs. Are these flywheel speeds technically aggressive? Yes – but two factors have to be kept in mind: First, these are imaginary CMGs, and are not the result of a mechanical design. Secondly, they are very aggressive, but not hopelessly so. The following considerations are important:

- This range of flywheel speed is at the edge of currently-demonstrated technology for high-speed flywheels. The region of a flywheel that is subjected to the greatest mechanical loads is the rim, and the perfomance of flywheels is frequently characterized by their "tip speed" the translational speed at the rim. Steel flywheels are limited to tip speeds of

Case Name	$\bar{q}$	*Control*	*Flywheel Speed*
L-C	50 psf	CMG-only	25000 rpm
L-A	50 psf	aero-only	25000 rpm
L-B	50 psf	both	25000 rpm
H-C	378 psf	CMG-only	33000 rpm
H-A	378 psf	aero-only	25000 rpm
H-B	378 psf	both	25000 rpm

Table 2: Simulation Cases

250-375m/s, depending on material properties. Composite energy storage flywheels have achieved approximately 2000m/s under laboratory conditions. Our tip speed at 25$krpm$ is roughly 1310m/s, and would be imposed under highly dynamic loads not typical of energy storage applications. Achieving a CMG flywheel with high tip speed will require, at the very least, a sophisticated design effort, and probably, additional technology development.

- The friction in conventional hydrostatic bearings scales linearly with the axle speed and to the fourth power with the journal diameter [9]. This may well present a significant mechanical issue in a system where support of very high-speed flywheels that are being rapidly gimballed to generate large torques with the roughly 5Hz bandwidth of the Dryden spectrum.

All of that said, the combination of CMG mass, size, and performance postulated in this paper are aggressive, but not likely impossible; moreover, we do not claim that these particular performance levels are even necessary. The six cases considered below are spot designs, rather than the result of formal full-system optimizations. It will be seen that the choice of time constant in (4) for cases L-B and H-B relegated the aero surfaces to an extremely undemanding role. Much work remains to be done in determining the most practical balance between CMGs and aero control.

For each of the six cases, a nominally straight and level trajectory was flown for 40 seconds, subject to disturbances from the Dryden turbulence model, each using an identical sequence of random numbers. Figures 1 and 2 display the results of these simulations. Note that in both Figures, circles are datapoint labels for aero-only cases H-A and L-A, squares for cases using combined aero and CMG control (or "Both") – H-B and L-B – and diamonds are used for cases using CMGs only – H-C and L-C. Low-$\bar{q}$ cases are plotted with dashed lines and high-$\bar{q}$ cases with solid lines. Each plot displays the temporal distribution of the variable being plotted by sorting the absolute value of the variable's time history into 20 bins and plotting the bin counts, normalized by the total number of time points in the simuation run. This gives the fraction of the simulation time during which the variable fell into each bin. Each could be viewed as having the same flavor as a probability density plot laid on its side.

Examining Figure 1, we see that all of the control scenari did well, and that the each of the six panels of the Figure tend to split into two clusters; in which one, corresponding to the "L" cases have significantly smaller errors and angular rates than the other, "H", cases. That's not a surprise, given that the disturbances are smaller. What is surprising is that the attitude performance appears to be less good when only aero effectors (the "-A" cases) are used.

This is particularly noticeable in the roll axis, where the angle and rate distributions lie well above the corresponding values for the -B and -C cases. One possible reason for this would be that the -A control designs weren't as good as the others – these are, after all, merely six point designs without a lot of time spent tuning. On the other hand, however, recall that we assumed ideal aero control effectors with no dynamics or saturation. We suspect, though a detailed analysis has not been performed, that the designs with active CMG (-B and -C) benefit from the angular momentum bias-induced gyric stiffness that was explored in [2] for the case where the angular momentum vector was stationary with respect to the body axes. In these cases, there's also a substantial angular momentum vector, though it's moving and changing magnitude; nonetheless, when crossed with the airframe angular vector, an internal torque is generated that dumps momentum into a direction orthogonal to each. Since the roll axis has the smallest moment of inertia, this benefit is most visible there. It should be stressed that this interpretation is merely well-informed speculation, and that the control algorithm was not structured to take advantage of this effect. The benefit, currently accidental, is significant enough to merit further study.

We now turn to Figure 2. Note that in this Figure, only the squares, corresponding to the -B cases, appear in all of the plots. The L-A traces are marked by very noisy use being made of the control surfaces – While rudder rates of nearly $300 deg/s$ and aileron rates in excess of $70 deg/s$ are not frequent in this case, they do repeatedly (and unrealistically) occur. The aero effector behavior in the -B cases, on the other hand, is on a dynamical par with that of trim devices: Very slow, very small deflections serve to assist the CMGs by gradually dumping angular momentum to avoid CMG saturation.

The gimbal torque and rate distributions are interesting. While roughly 99% of the H-B and H-C runs are spent with gimbal rates below $50 deg/s$, there's a substantial tail of instances where rates increase past $100 deg/s$. Similar behavior is seen in the gimbal torques, necessary for inducing the gimbal motion. This contrasts with the attitude behavior in the -B and -C cases, in Figure 1, where those cases produced the attitude rate profiles with the lowest distributions of angular rates.

An additional, very important, point is to recall from Table 2 that the flywheel speed for H-C is $33 krpm$, rather then $25 krpm$. We were unsuccessful in achieving a design that didn't saturate and blow up for the lower value. What's the significance of this?

- Even though our F16 model has approximately neutral static stability, it is still amazing that disturbance rejection and stabilization could be achieved, and to a very high degree, without imposing any external torques on the airframe. It should be noted that we were also able to obtain a successful L-C design, using a flywheel speed of $9 krpm$, rather than $25 krpm$. It provided almost identical distribution of attitude rates as the L-C in Figure 1, at the cost of more active CMGs, including a maximum gimbal rate excursion of roughly $100 deg/s$, and max gimbal torque of $150 Nm$. The gimbal agility was similar to that in H-C, while the torque output was lower because of the lower flywheel speed.

- The failure of the $25 krpm$ case highlights the importance of the tiny, slow, aero activity in performing the background desaturation of the CMGs as seen in the -B cases.

4 Conclusions

This paper documents an anecdotal exploration of two questions: First, is the notion of using CMGs in fixed-wind aircraft to augment its aerodynamic controls attractive? Second, what physical issues might arise in implementing such an augmentation? To examine these questions, we developed a common control system structure that can allocate control authority to aero effectors, a CMG array, or a frequency-partitioned blend of the two, and we looked at specimens of each of those three possibilities at two different steady, trimmed flight conditions. In each, the mission was to reject disturbances from heavy Dryden turbulence.

Regarding the first question, it was seen that, given our very superficial physical assumptions on the CMGs, they provided superior response to an idealized aerodynamic control system. We speculate that the superiority may be due to a level of gyric attitude stiffness present only when the CMGs were in use. The best performance was returned in the case where CMG and aero control worked together, with the aero effectors playing a very minimal direct role in the dynamics but, instead, keeping the CMGs desaturated. It should be noted that our CMG model was much more realistic than our aero model: The extremely precise attitude control that the CMGs achieved in our simulation is probably achievable with some configuration of CMG system.

Regarding the second question, the exact CMG system that we chose would have had minimal impact on the mass of its host aircraft, but would have posed design and technology difficulties, doubtless solvable. On the other hand, however, the control and CMG configuration for this study was entirely un-optimized. Further trades need to be conducted that balance between downsizing the aero machinery, and modulating the mass and technology assumptions on the CMG to find a more realistic design point for assessing the viability of such a system with reasonable-term technology. For example, the fact CMGs can generate large transient torques opens up contemplation of alternate technologies for aero moment generation that are bandwidth-limited but may have other advantages.

Further controls work needs to be done, particularly on large angular maneuvers. Our example aircraft was approximately neutral in its static stability. Would we do better with an airframe in which all three axes were unstable, and where stabilization consisted of dithering the CMG torques with the aircraft in equilibrium? Answers to these questions are reserved to future papers.

A Details of Flight Control Law

This appendix provides a detailed definition of the flight control system employed in this study. Following the notations as used in [10], the rotational equations of motion in the body frame are

$$\dot{h} + \omega^{\times} h = \tau_{\text{AERO}}(\bar{q}, \alpha, \beta, \delta_e, \delta_r, \delta_a) \tag{A.1}$$

where $\omega^{\times} h$ is the cross product of the airframe rotational velocity with the system angular momentum h. The $\delta_{(.)}$ are the aero control effector deflections, α is angle of attack, and β is

sideslip angle. The momentum h is

$$h = J(\eta)\omega + H \tag{A.2}$$

where $J(\eta)$ is the inertia of the airframe and CMG array, expressed in the body frame. Note the dependence on η, the four instantaneous gimbal angles. The quantity H is the CMG angular momentum due to $\dot{\eta}$ and Ω, given by

$$H = R_2^T I_C^g \dot{\eta} + (R_1(\eta))^T I_W^a \Omega \tag{A.3}$$

The first term, the contribution of the gimbal motion, transforms the four gimbal momenta $I_c^g \dot{\eta}$ from the individual gimbal rotational axes to the body frame via the direction cosine matrix $R_2 \in \mathcal{R}^{4\times 3}$. The second term transforms the four flywheel angular momenta $I_W^a \Omega$, expressed in their spin axes, to the body frame via $R_1(\eta)$.

Our flight control system treats the CMGs as external torquers so that

$$J(\eta)\dot{\omega} = \tau_{\text{AERO}} + u_{\text{CMG}} \tag{A.4}$$

where

$$u_{\text{CMG}} = -\dot{H} - \omega^{\times}(J(\eta)\omega + H) - \dot{J}(\eta)\omega \tag{A.5}$$

In order to realize u_{CMG} at the current η, differentiate (A.3) to obtain

$$R_2^T I_c^g \ddot{\eta} + \left(\omega^{\times} R_2^T I_c^g + A(\eta) + B(\eta,\omega)\right)\dot{\eta} = -u_{\text{CMG}} - \omega^{\times}(R_1(\eta))^T I_W^a \Omega - \omega^{\times} J(\eta)\omega \tag{A.6}$$

where

$$A(\eta) = [a_1 \ : \ \cdots \ : \ a_4], \quad a_i = \frac{\partial R_1^T}{\partial \eta_i} I_W^a \Omega \quad \text{AND} \quad B(\eta,\omega) = [b_1 \ : \ \cdot \ : \ b_4], \quad b_i = \frac{\partial J^T}{\partial \eta_i}\omega \tag{A.7}$$

A steering law based on a pseudoinverse solution is given as

$$\dot{\eta}^* = -[\omega^{\times} R_2^T I_c^g + A(\eta) + B(\eta,\omega)]^{+}\left(u_{\text{CMG}} + \omega^{\times}(R_1(\eta))^T I_W^a \Omega + \omega^{\times} J(\eta)\omega - R_2^T I_c^g \ddot{\eta}\right) \tag{A.8}$$

In order to avoid internal singularities in this type of pseudoinverse steering solution, a "singularity robust inverse" algorithm [11], [12], [13], is implemented. This modified algorithm adds a small positive increment to the pseudoinverse solution if it is detected that it is close to losing rank. The references cited are several of a larger number of versions of this general notion.

The following expression provides a tracking control law for gimbal torques τ_g that steer the CMGs toward the commanded $\dot{\eta}^*$ from (A.8). The absolute angular momenta of the CMGs along their gimbal axes is

$$h_{c_2} = I_c^g(\omega_2^\eta + \dot{\eta}) \tag{A.9}$$

where ω_2^η is the vector of projections of ω onto the gimbal axes of the individual CMGs in the array,

$$\omega_2^\eta = \begin{bmatrix} \omega_2^{\eta_1} \\ \vdots \\ \omega_2^{\eta_4} \end{bmatrix} \quad \text{where} \quad \begin{bmatrix} \omega_1^{\eta_i} \\ \vdots \\ \omega_3^{\eta_i} \end{bmatrix} = C_{G_i}(\eta_i) C_{G_i}^0 \omega, \quad i = 1, \ldots, 4 \tag{A.10}$$

and $C_{G_i}^0$ is the direction cosine matrix transforming body frame to CMG orientation at $\eta = 0$, and $C_{G_i}(\eta_i)$ transforms to current gimbal orientation. The dynamical equations for this portion of the CMG are

$$\left.\begin{array}{rcl} \dot{h}_{c_2} & = & \tau_g - \text{diag}\left\{\omega_3^\eta\right\}\left[(I_c^s - I_c^o)\omega_1^\eta + I_W^a \Omega\right] \\ & = & \tau_g - \tau_\omega \end{array}\right\} \tag{A.11}$$

where the definition of τ_ω is obvious from context, and where I_c^s is the moment of inertia of the entire flywheel/gimbal assembly along the spin axis, and I_c^o is the moment of inertia along the output axis. Define the torque command to the gimbal motors as

$$\tau_g = I_c^g\left[\dot{\omega}_2^\eta - 20\pi(\dot{\eta} - \dot{\eta}^*)\right] - \tau_\omega \tag{A.12}$$

The u_{AERO} command was translated into control surface deflections via the following logic:

$$\begin{bmatrix} \delta_e \\ \delta_r \\ \delta_a \end{bmatrix} = \begin{bmatrix} \hat{\delta}_e \\ \hat{\delta}_r \\ \hat{\delta}_a \end{bmatrix} + \frac{1}{\bar{q}S} C^{-1} \left[u_{\text{AERO}} - \left(\tau_{\text{AERO}}(\bar{q}, \alpha, \beta, 0, 0, 0) - \frac{\bar{q}}{\hat{\bar{q}}} \tau_{\text{AERO}}(\hat{\bar{q}}, \hat{\alpha}, \hat{\beta}, 0, 0, 0) \right) \right] \tag{A.13}$$

where $(\hat{\cdot})$ denotes trim quantities and

$$C = \begin{bmatrix} 0 & bC_{L_{\delta_r}} & bC_{L_{\delta_a}} \\ \bar{c}C_{M_{\delta_e}} & 0 & 0 \\ 0 & bC_{N^{\delta_r}} & bC_{N_{\delta_a}} \end{bmatrix} \tag{A.14}$$

As a final note, the MRP parameters from (2) obey the following governing equations:

$$\dot{\epsilon} = g(\epsilon)\omega \tag{A.15}$$

where

$$g(\epsilon) = \frac{1}{4}[(1 - \epsilon^T\epsilon)I + 2\epsilon^\times + 2\epsilon\epsilon^T] \tag{A.16}$$

Acknowledgements

The authors thank their colleagues Fred Lallman, Jay Brandon, and Dave Cox, of NASA Langley Research Center for helpful discussions and aid.

References

[1] Lim, K.B., Shin, J.Y., Cooper, E.G., and Moerder, D.D., "A new approach to attitude stability and control for low airspeed vehicles", AIAA Guidance, Navigation, and Control Conference and Exhibit, August 16-19, 2004, Providence, RI. AIAA Paper 2004-5008.

[2] Lim, K.B., Shin, J.Y., and Moerder, D.D., "Bias momentum sizing for hovering dual-spin platforms", AIAA Paper 2005-5973 and NASA/TP-2006-214317.

[3] Lim, K.B., Shin, J.Y., and Moerder, D.D., "Variable speed CMG control of a dual-spin stabilized unconventional VTOL air vehicle," AIAA 3rd *Unmanned Unlimited* Technical Conference, Workshop & Exhibit, September 20-23, 2004, Chicago, IL, AIAA Paper 2004-6537.

[4] Wie, B., *Spacecraft Vehicle Dynamics and Control*, 1998, AIAA Education Series, AIAA Inc., Reston, Virginia.

[5] *Spacecraft Attitude Determination and Control*, James R. Wertz, editor, Kluwer Academic Publisher, Boston, 1978.

[6] *MIL-STD-1797A*.

[7] Stevens, B.L., and Lewis, F.L., *Aircraft Control and Simulation*, John Wiley & Sons, Inc, New York, 1992.

[8] Junkins, J.L., "Adventures on the Interface of Dynamics and Control," *Theodore von Karman Lecture*, AIAA Aerospace Sciences Meeting, Reno, Nevada, January 1997.

[9] Stolarski, T. A., *Tribology in Machine Design*, Elsevier, 2000.

[10] Hughes, P.C., *Spacecraft Attitude Dynamics*, John Wiley & Sons, New York, 1986.

[11] Bedrossian, N.S., Paradiso, J., Bergmann, E.V., and Rowell, D., "Steering Law Design for Redundant Single-Gimbal Control Moment Gyroscopes," *Journal of Guidance, Control, and Dynamics*, Vol. 13, No. 6, 1990, pp. 1083-1089.

[12] Bedrossian, N.S., Paradiso, J., and Bergmann, E.V., "Redundant single gimbal control moment gyroscope singularity analysis," *Journal of Guidance, Control, and Dynamics*, Vol. 13, No. 6, 1990, pp. 1096-1101.

[13] Schiehlen, W.O., "Two different approaches for a control law of a single gimbal control moment gyro systems," NASA TM X-64693, August 1972.

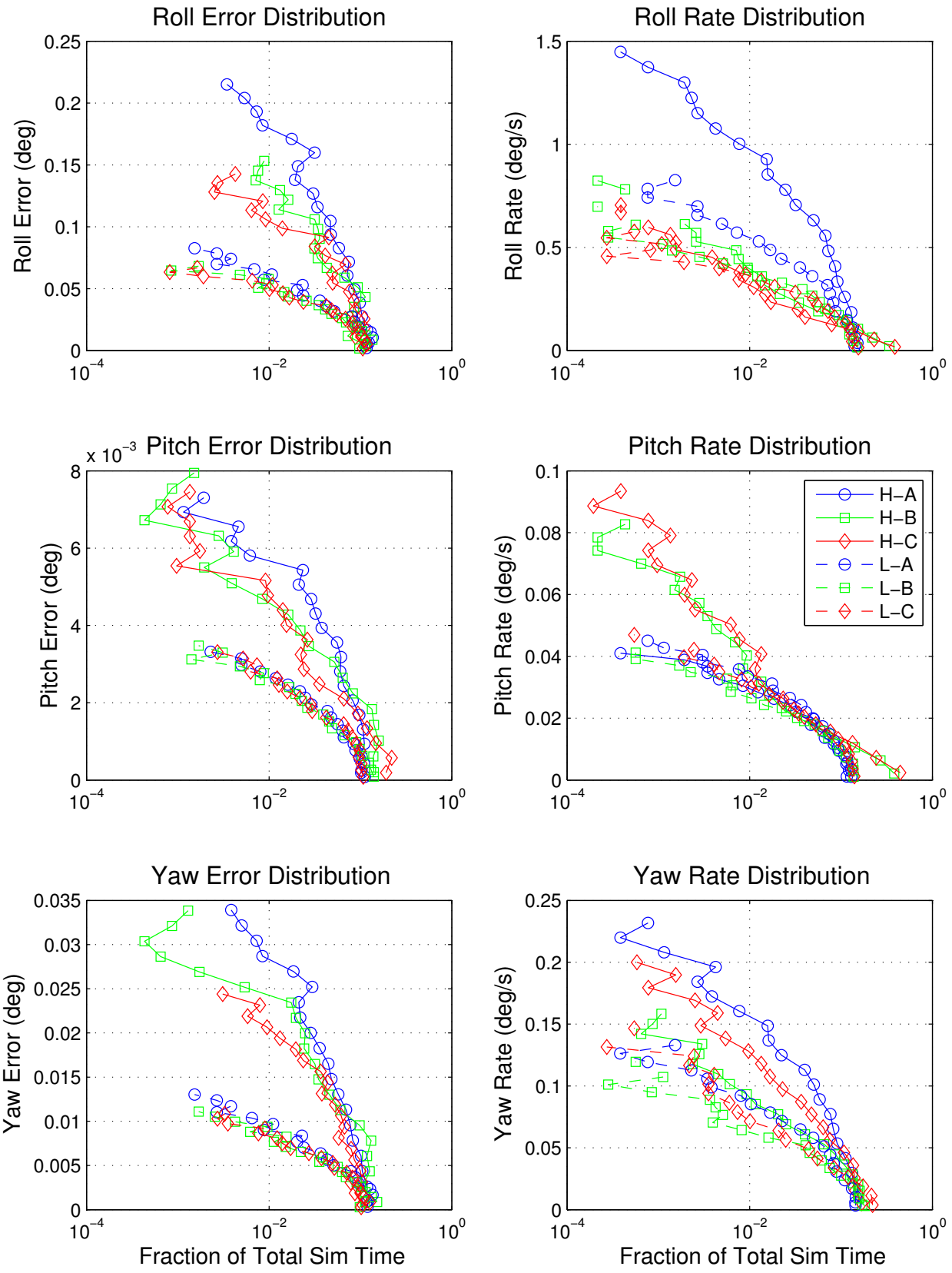

Figure 1: Distribution of Attitude Errors and Rates in Six Cases

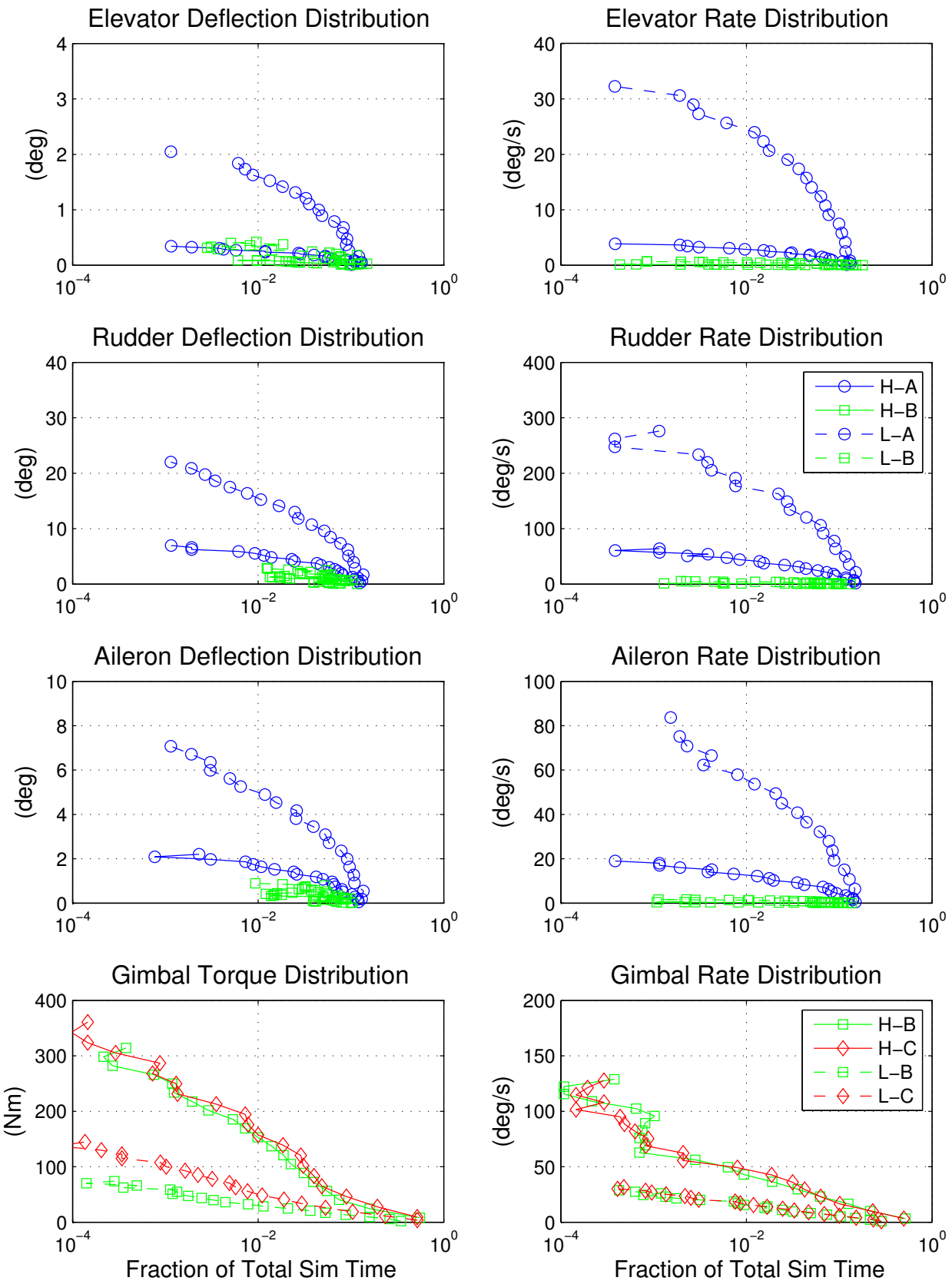

Figure 2: Distribution of Controls Commands and Rates in Six Cases